Experimental Parasitology 151-152 (2015) 56–63

Contents lists available at ScienceDirect

Experimental Parasitology

journal homepage: www.elsevier.com/locate/yexpr

Full length article

Prediction of substrate specificity and preliminary kinetic characterization of the hypothetical protein PVX_123945 from *Plasmodium vivax*

Bharath Srinivasan [1], Lakshmeesha Kempaiah Nagappa [2], Arpit Shukla [2], Hemalatha Balaram *

Molecular Biology and Genetics Unit, Jawaharlal Nehru Centre for Advanced Scientific Research, Jakkur, Bangalore 560 064, Karnataka, India

HIGHLIGHTS

- PVX_123945 was predicted to be a phosphatase using various in silico analyses.
- Kinetics validated prediction, showed specificity for β-glycerophosphate and pyridoxal 5′-phosphate.
- First attempt at biochemical characterization of a hypothetical HAD superfamily member from *P. vivax*.

GRAPHICAL ABSTRACT

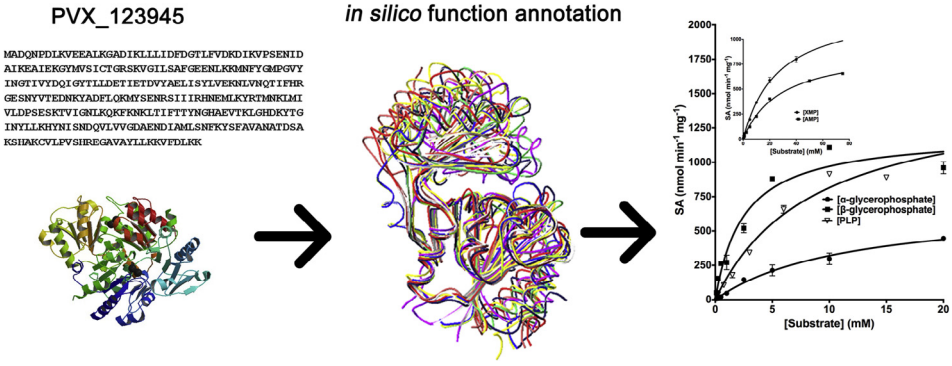

ARTICLE INFO

Article history:
Received 29 June 2014
Received in revised form 12 January 2015
Accepted 27 January 2015
Available online 2 February 2015

Keywords:
Hypothetical protein
In silico function annotation
Multiple-structure alignment
Docking
Substrate screen
Phosphatase
Sugar hydrolase

ABSTRACT

Members of the haloacid dehalogenase (HAD) superfamily are emerging as an important group of enzymes by virtue of their role in diverse chemical reactions. In different *Plasmodium* species their number varies from 16 to 21. One of the HAD superfamily members, PVX_123945, a hypothetical protein from *Plasmodium vivax*, was selected for examining its substrate specificity. Based on distant homology searches and structure comparisons, it was predicted to be a phosphatase. Thirty-eight metabolites were screened to identify potential substrates. Further, to validate the prediction, biochemical and kinetic studies were carried out that showed that the protein was a monomer with high catalytic efficiency for β-glycerophosphate followed by pyridoxal 5′-phosphate. The enzyme also exhibited moderate catalytic efficiencies for α-glycerophosphate, xanthosine 5′-monophosphate and adenosine 5′-monophosphate. It also hydrolyzed the artificial substrate p-nitrophenyl phosphate (pNPP). Mg^{2+} was the most preferred divalent cation and phosphate inhibited the enzyme activity. The study is the first attempt at understanding the substrate specificity of a hypothetical protein belonging to HAD superfamily from the malarial parasite *P. vivax*.

© 2015 Elsevier Inc. All rights reserved.

Abbreviations: HAD, haloacid dehalogenase; EDTA, ethylenediaminetetraacetic acid; SDS–PAGE, sodium dodecyl sulphate–polyacrylamide gel electrophoresis; pNPP, p-nitrophenyl phosphate.

* Corresponding author. Fax: +91 80 22082766.
Email address: hb@jncasr.ac.in (H. Balaram).
[1] Present address: Center for the Study of Systems Biology, 250 14th Street, NW, Room 109, Atlanta, GA 30318, USA.
[2] Have contributed equally to this work.

http://dx.doi.org/10.1016/j.exppara.2015.01.013
0014-4894/© 2015 Elsevier Inc. All rights reserved.

1. Introduction

Sequencing of several genomes has yielded numerous predicted open reading frames (ORF) to which functions cannot be readily assigned. These proteins, either orphan hypothetical proteins or conserved hypothetical proteins, comprise almost 20–40% of proteins encoded in each newly sequenced genome (Galperin, 2001). Hypothetical proteins pose a challenge to general biology in terms of understanding their role in cellular function. There are several different approaches to annotate function to hypothetical proteins. Genetic, biochemical and computational tools are routinely applied in arriving at the function of such hypothetical proteins. Structural genomics initiatives, by determining the three-dimensional structure of orphan hypothetical proteins, are trying to annotate function by understanding the unique attributes of a protein structure such as the nature and mode of prosthetic group/metal ion binding, possible clues about catalytic and regulatory sites and the fold similarity with other proteins of known functions (Eisenstein et al., 2000).

P. vivax, the causative agent of benign malaria with approximately 70–80 million cases annually (Mendis et al., 2001), is poorly studied compared to *Plasmodium falciparum*. Unlike the *P. falciparum* genome, which is 19.4% G + C rich and 60.5% of the predicted proteins are hypothetical, *P. vivax* is 42.3% G + C rich and only 36% of the predicted proteome is hypothetical (Carlton et al., 2008; Gardner et al., 2002; Acharya et al., 2011). Annotating biochemical function to these hypothetical proteins would enable better understanding of the parasite biology to evolve effective intervention strategies. For the current study, we have selected a hypothetical protein which is a member of the HAD superfamily of enzymes.

Haloacid dehalogenases (HAD) are a vast superfamily of largely uncharacterized enzymes containing more than 3000 members from various kingdoms of life. Characteristic structural features for members of HAD superfamily are the presence of an α/β core and a cap domain. The core domain has a Rossmanoid fold. The presence, location and structure of the cap domain permit classification of HADs into 3 distinct subfamilies viz., types I, II and III (Allen and Dunaway-Mariano, 2004). The cap domain in type I and II subfamilies comprises of an all α bundle and an α/β sandwich respectively, while proteins in subfamily III lack the cap altogether (Burroughs et al., 2006). The cap is inserted between loops 1 and 2 of core domain in type I and between loops 2 and 3 in type II HAD subfamilies. The active site located in the core domain is formed by four loops, which position substrate and cofactor binding residues as well as the catalytic groups that mediate the core chemistry. The four motifs typical of HAD superfamily members are motif I, which is DXDXV/T (where X is any of the twenty different amino acids), motif II, which is ΦΦΦT/S (where Φ is a hydrophobic residue), motif III containing an invariable lysine and motif IV containing one or two aspartates that might either be sequentially proximal or separated by three or four residues.

Understanding the structural features that contribute to substrate specificity is a main focus of ongoing work on members of HAD superfamily from various sources and this work is an additional effort at attempting to annotate the function of a HAD superfamily member. HAD superfamily members, in general, are known to act on a wide range of substrates. There are ample examples in literature showing the broad substrate and co-factor specificity of HAD superfamily members (Lu et al., 2005; Nguyen et al., 2008; Huang et al., 2011; Lu et al., 2011). In one study on a HAD superfamily member, BT4131, it was shown that the enzyme can utilize several divalent metal-ion cofactors and different sugar phosphates as substrates with varying k_{cat} and K_m values (Lu et al., 2005). In yet another paper on HAD phosphohydrolase BT1666, it has been shown that the enzyme possesses broad and overlapping substrate specificity with BT4131 (Lu et al., 2011). A recent paper on understanding the substrate specificity of a HAD superfamily member from *Bacteroides thetaiotaomicron* (BT2127) resorted to structure determination, substrate screen and site-directed mutagenesis to show that the protein functions as an inorganic pyrophosphatase and also assists in protein synthesis by removal of the product pyrophosphate from tRNA synthase (Huang et al., 2011).

The present study is an attempt at sequence and structure based function annotation of PVX_123945, a hypothetical protein from *P. vivax* belonging to the HAD superfamily of hydrolases class IIb. Bioinformatic analysis shows that the enzyme is a phosphatase. Biochemical and kinetic characterization, apart from validating the prediction, additionally demonstrates that the enzyme exhibits specificity for β-glycerophosphate and pyridoxal 5′-phosphate, with low levels of activity on α-glycerophosphate, AMP and XMP.

2. Materials and methods

2.1. Reagents

All the chemicals were of highest quality and, unless indicated otherwise, were obtained from Sigma-Aldrich, USA. Expression clone of PVX_123945 (PDB ID: 2B30), a hypothetical protein from *Plasmodium vivax*, was a kind gift from the Structural Genomics of Pathogenic Protozoa (SGPP) consortium, Seattle, Washington.

2.2. Bioinformatics analysis

The sequence of PVX_123945 and other HAD superfamily members were downloaded from GeneDB database. The non-redundant database at NCBI was used to search for homologs of PVX_123945 using the algorithm BLASTP. Distant homology searches were carried out using PSI-BLAST (Altschul et al., 1997). T-Coffee (http://www.ebi.ac.uk/t-coffee/) (Notredame et al., 2000) was used for generating multiple sequence alignment profiles. The protein sequence of different HAD superfamily members was submitted to servers nFOLD and mGenTHREADER (Jones, 1999) for fold recognition and initial pairwise alignment of the query sequence with the ten most suitable templates. Phylogenetic and molecular evolutionary analyses were done using MEGA version 3.1 (Kumar et al., 1994). The coordinate file for the structure of 2B30 was downloaded from the database maintained by the research collaboratory for structural bioinformatics (http://www.rcsb.org) (Bernstein et al., 1977). The coordinates of the query protein structure were submitted to the Dali server (http://www.ebi.ac.uk/dali/) that compares them against the coordinates of protein structures deposited in PDB (protein data bank) and reports back a multiple alignment of structural neighbors. Further pairwise structure alignments were carried out using the DaliLite server (ebi.ac.uk/DaliLite/) (Holm and Park, 2000). POSA (fatcat.burnham.org/POSA/) was also utilized to generate the multiple structure alignment profiles. Molecular visualization and structure analysis were done using various tools such as Swiss-PdbViewer (expasy.org/spdbv/) (Guex and Peitsch, 1997), PyMOL (pymol.sourceforge.net/) and CCP4 (Collaborative Computational Project no. 4) suite of programs (http://www.ccp4.ac.uk/download.php). Autodock 4.2 was used to carry out docking simulations (Morris et al., 2008). Lamarckian genetic algorithm (LGA) was used to compute the lowest energy of the system with linear free energy model of molecular mechanics terms. This included van der Waals interactions, directional hydrogen bonding, an empirical term that estimates the loss of torsional entropy of the ligand upon binding, screened Columbic electrostatics, and an atomic solvation parameter-based desolvation free energy term. More than 90% of the best-docked structures had the ligands correctly docked in the PVX_123945 active site.

2.3. Expression and purification of PVX_123945

The expression clone of PVX_123945 (PDB ID: 2B30), a putative HAD/COF like hydrolase from *P. vivax*, was provided to us cloned in plasmid BG1861 (a modified pET 14b vector) with an amino terminus hexahistidine tag. The recombinant plasmid DNA was used to transform competent *E. coli* BL21 (DE3) cells. The transformed cells were grown at 37 °C overnight and used as preinoculum for 800 ml terrific broth containing 100 μg/ml ampicillin. The cells were allowed to grow at 37 °C until the $O.D_{600}$ reached 0.6 and then were induced for 8 hours at 18 °C with isopropyl β-D-thiogalactopyranoside (IPTG) at a final concentration of 0.3 mM. The cells were harvested by centrifugation for 15 min. at 4 °C. The cell pellet was resuspended in 30 ml lysis buffer (50 mM Tris–HCl, pH 7.4, 100 mM NaCl, 10% glycerol, 2 mM DTT) and lysed by passing the cell suspension thrice through French press (1000 psi) (ThermoIEC, Thermo Fischer Scientific Inc., San Diego, CA, USA). The cell lysate was centrifuged at 16,000 rpm for 45 min at 4 °C. The supernatant was kept for binding with 800 μl of lysis buffer-equilibrated Ni–NTA beads (Novagen, EMD Chemicals, USA) for 3 hours at 4 °C. The histidine tagged protein bound beads were washed with lysis buffer containing 10 mM and 20 mM imidazole to wash off non-specifically bound protein. The protein was eluted with 250 mM imidazole and dialyzed against dialysis buffer (50 mM Tris–HCl, pH 7.4, 100 ml NaCl, 10% glycerol and 2 mM DTT) to remove imidazole. The dialyzed protein sample was concentrated at 4 °C using a 10K Microsep® centrifugal device (PALL Corporation, NY, USA) and stored at –20 °C. The protein was shown to be homogenous by SDS–PAGE (Laemmli, 1970) with a yield of 10 mg/800 ml of culture. Protein concentration was determined by the method of Bradford (1976) with bovine serum albumin (BSA) as protein standard.

2.4. Subunit molecular mass determination and oligomeric status

The theoretical molecular mass of the protein was calculated with the web utility ProtParam and the experimental molecular mass was determined by MALDI (matrix-assisted laser-desorption ionization) mass spectrometry (Ultraflex II, BruckerDaltonics, Germany). The protein sample for mass determination was dialyzed against water, 1 μl of protein (2 μg) was mixed with sinapinic acid (0.1 g of sinapinic acid in 0.5 ml of 50% acetonitrile and 0.1% trifluoroacetic acid) in 1:1 ratio, spotted on the MALDI target plate and mass spectra were recorded in the positive ion mode. The identity of the protein was further confirmed by Western blot analysis with anti-His antibodies.

The oligomeric status of the protein was probed by size-exclusion chromatography on an analytical Superdex 200 column (1 cm × 30 cm) attached to an AKTA Basic HPLC system. The column was equilibrated with buffer A (50 mM Tris–HCl, pH 7.4, 100 mM NaCl and 1 mM EDTA) and calibrated using molecular weight standards, β-amylase (200 kDa), alcohol dehydrogenase (150 kDa), bovine serum albumin (66 kDa), carbonic anhydrase (29 kDa) and cytochrome c (12.4 kDa). The flow rate was maintained at 0.5 ml min^{-1}. Purified protein (20 μM) was loaded on the column and the elution was monitored at 280 nm. The native mass was obtained from a plot of the logarithm of molecular mass of standards vs. their elution volume from the column.

2.5. Activity assays

One continuous assay and one end point assay were utilized to derive kinetic parameters. The rate of *p*-nitrophenyl phosphate (pNPP) hydrolysis was determined by monitoring the increase in absorbance at 405 nm (molar extinction coefficient (ε) of pNPP is 18,000 M^{-1} cm^{-1}) at 27 °C. One milliliter of assay mixture contained 50 mM Tris–HCl, pH 8.0, 20 mM $MgCl_2$ and various concentrations of pNPP. The concentration of enzyme was 730 nM. The reaction was monitored for a minimum of 10 minutes for getting reliable slopes.

Except pNPP, phosphate ester hydrolysis for the other substrates was monitored using Chen's assay (Chen et al., 1956), which is an end point measurement. Two hundred microliters of reaction volume contained 50 mM Tris–HCl, pH 7.4, 20 mM $MgCl_2$ and 730 nM enzyme. The reaction was initiated by addition of varying concentration of the respective substrates and allowed to proceed for 30 min at 27 °C. The reaction was quenched by addition of 20 μl of 70% TCA. The reaction mix was centrifuged at 13,000 rpm for 10 min and 100 μl of the supernatant was added to 1 ml of Chen's reagent (6N sulphuric acid, distilled water, 2.5% ammonium molybdate and 10% ascorbic acid mixed in 1:2:1:1 ratio). The reaction mix was allowed to incubate at 37 °C for 30 min for color stabilization and absorbance was recorded at 820 nm (molar extinction coefficient (ε) is 25,000 M^{-1} cm^{-1}).

All the assays were carried out under initial velocity conditions where the product formed was less than 5% of the initial substrate concentration. Further, it was ensured that the assays were carried out within linear ranges with respect to enzyme concentration and during the linear timeframe of product formation. Each experiment was carried out in triplicate.

To ascertain whether the enzyme acts on a particular substrate, 5 mM of each substrate was tested. Subsequently, to determine the K_m of substrates on which the enzyme acts, they were titrated at fixed saturating concentration of Mg^{2+} (30 mM) and the resultant velocities were plotted against substrate concentration and fit to the Michaelis–Menten equation (1). The concentration of enzyme used was 730 nM. Assuming Mg^{2+} to be a pseudo-substrate, its dissociation constant was determined by titrating it at saturating concentration of pNPP (15 mM). The data were fit to equation (1).

$$v = (V_{max} \times [S])/(K_m + [S]) \quad (1)$$

where v is velocity of the enzyme, V_{max} is maximum velocity, [S] is substrate concentration, K_m is the Michaelis–Menten constant for pNPP/metal ion.

Product inhibition studies on the protein, PVX_123945, were carried out by performing continuous assays with saturating [Mg^{2+}] and varying [pNPP] at several fixed concentration of the product Pi. Another study was carried out whereby Mg^{2+} was varied at several fixed concentrations of phosphate and saturating pNPP. The data were fit to equation (2) using GraphPad Prism version 4 (GraphPad Software, Inc., San Diego, CA)

$$v = V_{max} \times [S]/[K_m \times (1 + I/K_i) + [S]] \quad (2)$$

where I is the concentration of the inhibitor and K_i is the inhibition constant. Unless mentioned otherwise, all the data were fit using linear regression and non-linear curve fitting subroutines of GraphPad Prism, version 4.0 (GraphPad Software, Inc., San Diego, CA).

2.6. Metal dependence

The metal cofactor specificity was examined using pNPP as substrate for PVX_123945. Reaction solutions contained 730 nM enzyme, 50 mM Tris–HCl, pH 8.0 and saturating concentration of pNPP (30 mM) were taken and various metal ions such as $MnCl_2$, $MgCl_2$, $CaCl_2$, $CoCl_2$, and $ZnCl_2$ were titrated to test for their effect on enzyme activity. To study the effect of monovalent cations, the reaction mix containing 50 mM Tris–HCl, pH 8.0, and 730 nM of enzyme was titrated with monovalent cations such as NaCl and KCl.

Table 1
Haloacid dehalogenase members in the annotated genome sequence of *Plasmodium vivax*.

S. no.	Type	Member id[#]	Annotation for *P. vivax* protein	Protein length
1.	ATPase	PVX_081455 (PfATP6)	Calcium transporting ATPase, putative	1196
		PVX_084625 (PfATP4)	P-type ATPase, putative	1355
		PVX_123800 (PF3D7_1223400)	Phospholipid transporting ATPase, putative	1680
		PVX_092535 (PfGCalpha)	Adenylate/Guanylate cyclase catalytic domain, putative	3979
		PVX_081695 (PF3D7_0727800)	Cation-transporting ATPase, putative	1678
		PVX_123625 (PfATPase2)	Aminophospholipid-transporting ATPase, putative	1514
		PVX_098690 (PfCuTP)	Cation-transporting ATPase, putative	2073
		PVX_095285 (PfATPase7)	Phospholipid-transporting ATPase, putative	1707
2.	Hypothetical proteins and sugar phosphatases	PVX_123945 (PfHAD2)	Haloacid dehalogenase-like hydrolase, putative	293
		PVX_111055 (PfHAD1)	Sugar phosphatase, putative	292
		PVX_123935 (PfHAD3)	Haloacid dehalogenase like hydrolase, putative	336
		PVX_122960 (PfPNPase)	Phosphoglycolate phosphatase precursor, putative	314
		PVX_091555 (PfHAD4)	Haloacid dehalogenase-like hydrolase, putative	303
		PVX_001740 (PfPMM)	Phosphomannomutase, putative	246
3.	Nucleotidase	PVX_084340 (PF3D7_1206100)	IMP-specific 5′-nucleotidase, putative	444
4.	Others	PVX_114760 (PfNIF3)	NLI interacting factor-like phosphatase, putative	1544
		PVX_117035 (PF3D7_1468600)	Phospholipid-transporting ATPase, putative	1882

Numbers in parentheses are the *Plasmodium falciparum* IDs.

3. Results

3.1. *HAD members in* Plasmodium

Annotations assigned by Pfam and PlasmoDB databases, distant homology searches (PSI-BLAST) followed by multiple sequence alignment, conserved motif search and threading indicate that 17 HAD superfamily members are present in *P. vivax* (Table 1) while there are 20 of them in *P. falciparum*. This number includes proteins with multiple domains with at least one domain sharing features typical of HAD superfamily members.

All other species under Plasmodia, e.g. *P. knowlesi, P. cynomolgi, P. yoelii, P. berghei* and *P. chabaudi*, have HAD members anywhere between 16 and 20. Two HAD members are notable exceptions by being altogether absent in the murine malaria causing species of Plasmodia (an IMP-specific 5′-nucleotidase and a putative aminophospholipid transporter) (Frech and Chen, 2011; Srinivasan and Balaram, 2007). The absence of these proteins from pathogens causing rodent malaria might be reflective of the specificity of metabolic requirement depending on the host.

3.2. *In silico function annotation of PVX_123945*

PVX_123945 is a hypothetical protein of HAD superfamily subfamily IIb. All the motifs characteristic of HAD superfamily hydrolase are conserved in this protein. Homologs of this protein are present in all species of *Plasmodium* whose genome sequences are available. Since HAD superfamily members are shown to be involved in several pivotal functions in other organisms, functional annotation of this protein in *P. vivax* might contribute toward furthering our understanding of the parasite metabolism. When the sequence of PVX_123945 was queried against the non-redundant database at NCBI, several hypothetical proteins belonging to HAD subfamily IIb from a diverse set of protozoans and bacteria were retrieved. PVX_123945 does not have any homologs in humans. In the absence of any known sequence homologs whose functions were known, the structure of the protein PVX_123945 (PDB ID: 2B30) was submitted for structure–structure alignment using the Dali server against the whole PDB structure database. The results indicated that there were several structures with Z-scores greater than 6.0. Because HAD superfamily members share a highly conserved core domain, the “hits” represent all three subfamilies representing different cap architectures. These structures share 10–23% overall amino acid sequence identity and root mean square deviation of 2.2–6.1 Å when aligned with 2B30. The HAD structures having the highest Z-scores were, however, those which shared cap topology with 2B30 and assumed the same domain–domain conformation (i.e. open vs. closed). The most closely related folds were those of HAD members which were sugar phosphate phosphatases, especially 1YMQ ($Z = 29.5$), a subclass IIb HAD enzyme. A representative set of hits from the DALI search are summarized in Table 2 and the multiple structure alignment of those structures is shown in Fig. 1A.

Structural superposition of 2B30, sucrose-6-phosphate phosphatase and pyrimidine 5′-nucleotidase indicates that the hypothetical protein resembles sugar phosphate phosphatase fold more than a pyrimidine 5′-nucleotidase fold (Fig. 1B). Further, macromolecular rigid-body docking of substrates using AutoDock 4 indicated that the active site could accommodate substrates ranging from very small ones (like pyridoxal 5′-phosphate) to intermediate-sized substrates (glucose-6-phosphate). In the case of PLP, more than 90% of the docked conformations were in the active site with an average ΔG of –7.5 kcal mol^{-1} (Fig. S1A and B). From Dali search

Table 2
A representative set of Dali search results of the PDB database for function annotation of PVX_123945 (PDB ID: 2B30) that guided the substrate screen.

S. no	PDB ID	Z[#]	RMSD[a]	% ID[b]	annotation
1	1rlm	30.5	2.2	22	Phosphatase[1]
2	1ymq	29.5	2.2	22	Sugar phosphate phosphatase BT4131[1]
3	1nf2	27.0	2.9	21	Phosphatase, unknown function[2]
4	2hf2	24.2	3.6	22	Sugar phosphatase SUPH[2]
5	3nrj	20.1	2.1	22	Probable YRB1 family phosphatase[2]
6	2r8x	19.6	2.3	22	3-deoxy-D-manno-octulosonate 8-phosphate phosphatase[1]
7	1u2s	19.2	3.2	19	Sucrose phosphatase[1]
8	3ewi	19.1	2	19	Phosphatase domain with no activity[1]
9	1wzc	18.4	3.1	17	Mannosyl-3-phosphoglycerate phosphatase[1]
10	2i54	18.4	2.3	17	Phosphomannomutase[1]
11	1tj3	18.0	3.2	19	sucrose phosphate phosphatase (SPP)[1]
12	1u02	16.2	4.0	16	Trehalose-6-phosphate phosphatase[1]

[#] Structural alignment score normalized by the length of alignment.
[a] RMSD, root mean square deviation.
[b] % ID, percentage identity between the sequence of the query and the hits.
[1] Experimentally characterized activities.
[2] Predicted activities.

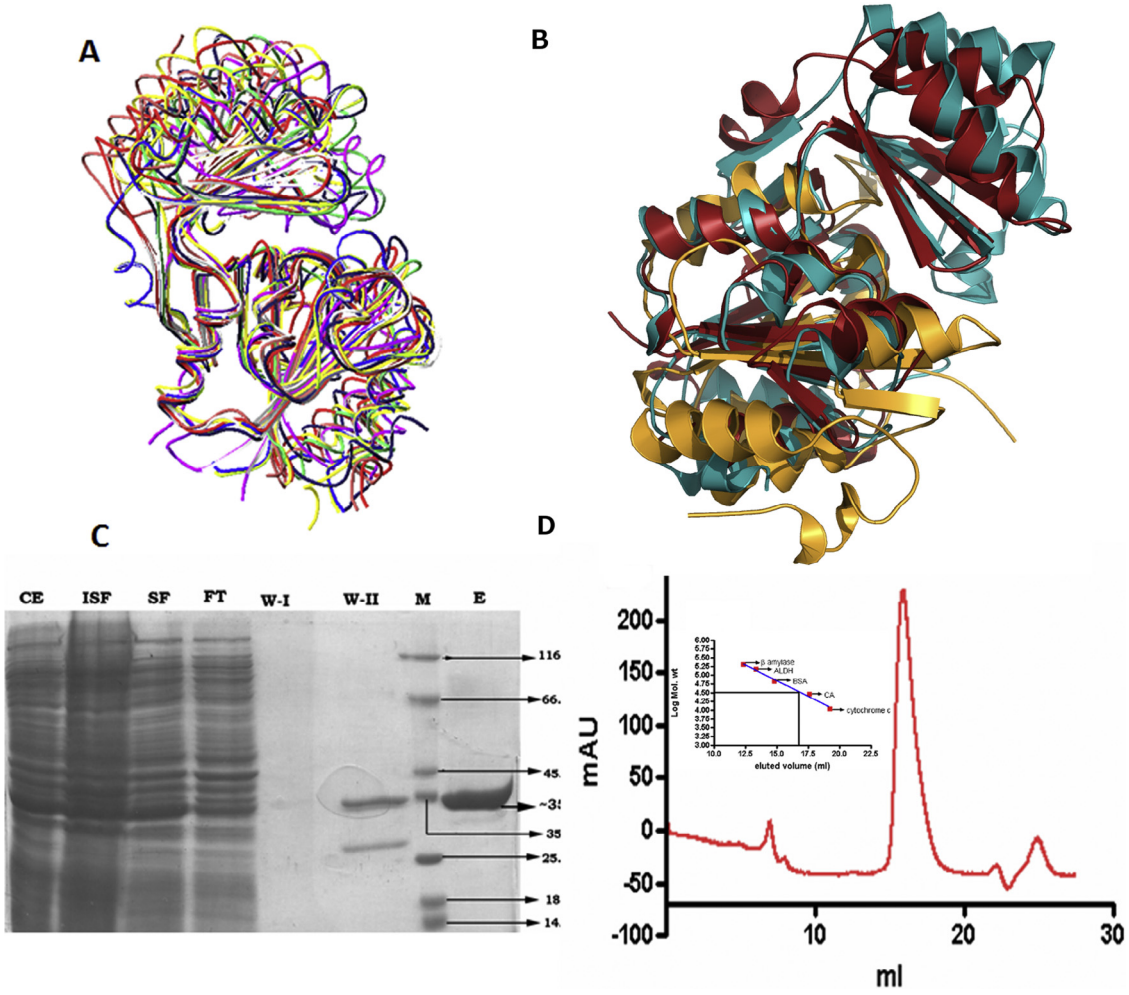

Fig. 1. (A) High overall fold conservation of various HAD sugar phosphate phosphatases in spite of low sequence identity. 1nf2, yellow; 1rlm, red; 1tj3, blue; 1u2s, light green; 1wzc, pink; 1ymq, deep green, 2hf2, brown; 2b30, navy blue. The structures were selected from the Dali search results and aligned using Swiss-PdbViewer (Altschul et al., 1997). The structures are represented as licorice for ease of visualization. (B) Multiple structure superposition of the PDB IDs 2B30 (teal), 1TJ5 (burnt umber), and 2BDU (saffron) structures. Figure shows the fragment of structures that superposes well. Structures are shown in cartoon representation. 2B30 is a hypothetical protein from *P. vivax*, 1TJ5 is sucrose-6-phosphate phosphatase from *Synechocystis sp.*, and 2BDU is a pyrimidine 5′-nucleotidase from *Mus musculus*. The alignments and figure were generated using POSA multiple structure alignment server (fatcat.burnham.org/POSA/) and MacPyMol, respectively. (C) Expression and purification of PVX_123945. CE, crude extract; ISF, insoluble fraction, SF, soluble fraction; FT, Flow-through; WI, wash I; W-II, wash II; M, molecular weight marker; E, eluant. Molecular weight, in kDa, of the protein standards is indicated to the left of the gel. (D) The oligomeric status of the protein probed by size-exclusion chromatography. The figure shows the elution profile of the protein and the inset shows the elution of standards. Molecular weight standards are β-amylase (200 kDa), alcohol dehydrogenase (150 kDa) (ADH), bovine serum albumin (66 kDa) (BSA), carbonic anhydrase (29 kDa) (CA) and cytochrome c (12.4 kDa). (For interpretation of the references to color in this figure legend, the reader is referred to the web version of this article.)

results, sequence alignment, pairwise structure alignment and docking analysis, it was predicted that PVX_123945 is a phosphatase with possible activity toward sugar phosphates.

3.3. Biochemical and kinetic analysis of PVX_123945

To validate the prediction biochemically, the protein was expressed and purified to homogeneity by immobilized nickel affinity chromatography (Fig. 1C). The identity of the protein was confirmed by ascertaining its mass using MALDI mass-spectrometry and Western blotting with anti-histidine antibodies (Fig. S2A and S2B). On the analytical size-exclusion chromatography column, the protein eluted at a volume corresponding to a monomer (Fig. 1D). Observed hydrolysis of the artificial substrate pNPP to pNP and phosphate supported the prediction that the protein was a phosphatase (Fig. 2A). Various monovalent (Na^+, K^+ and Li^+) and divalent ions (Ca^{2+}, Co^{2+}, Mg^{2+}, Mn^{2+} and Zn^{2+}) were titrated at saturating concentration of pNPP to evaluate their effect on enzyme activity. The reverse, whereby pNPP was titrated in the presence of various divalent cations, was also carried out. Except for Mg^{2+} and Mn^{2+}, and to a lesser extent Co^{2+}, the other divalent ions did not serve as cofactors in the pNPP hydrolysis activity of the enzyme (Fig. 2B). On the contrary, monovalent ions had little effect on enzyme activity. Metal ions, at saturating pNPP concentration, behaved as pseudosubstrates and gave hyperbolic plots from which kinetics constants were estimated. Mg^{2+} had a K_m value of 0.14 ± 0.01 mM and a V_{max} value of 3.6 ± 0.8 nmol min^{-1} mg^{-1} while Mn^{2+} had a K_m value of 1.21 ± 0.32 mM and a V_{max} value of 3.74 ± 0.72 nmol min^{-1} mg^{-1}. The higher affinity of the enzyme for Mg^{2+} suggests that it must be the physiologically relevant metal ion cofactor. Purified PVX_123945 (non-EDTA treated) shows residual pNPP hydrolysis activity indicative of co-purification of the enzyme with metal cofactor. PVX_123945 activated with Mg^{2+} was found to catalyze the hydrolysis of pNPP with reasonable efficiency [$k_{cat}/K_m = 3.0 \times 10^{-3}$ mM^{-1} s^{-1} (Table 3)]. Phosphate inhibited the pNPP hydrolyzing activity of the enzyme with an IC-50 of 0.27 ± 0.07 mM and product inhibition plots

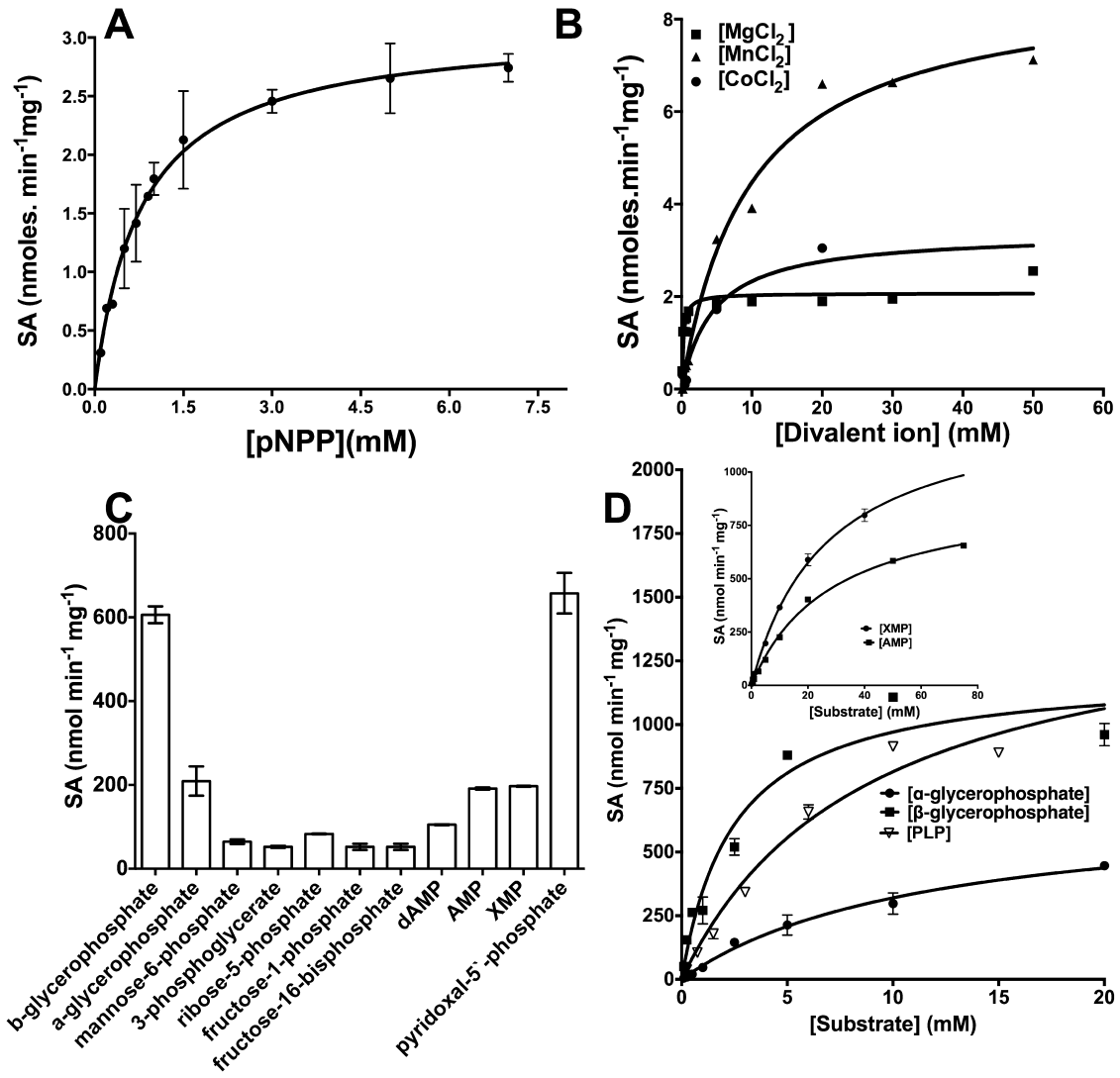

Fig. 2. (A) Substrate vs. activity plot for pNPP hydrolysis indicative of phosphatase activity. (B) Superposition of divalent metal ion titration vs. activity plots at saturating concentration of substrate pNPP. The assay condition was 50 mM Tris, pH 8.0, 15 mM pNPP and variable metal ions. The activity was measured by quantifying the amount of pNP formation at 405 nm. (C) Histogram showing the screen for potential substrates of PVX_123945. Shown only are substrates that exhibited a specific activity value of 50 nmol min^{-1} mg^{-1} or above. A total of 38 substrates were included in the screen. Substrates whose specific activity values were below this cut-off are NAD, dGMP, 2-phosphoglycerate, glucose-6-phosphate, glucose-1-phosphate, fructose-6-phosphate, fructose-1, 6-bisphosphate, 2,3-bisphosphoglycerate, TMP, IMP, dIMP, CMP, UMP, 3′-AMP, phosphoenol-pyruvate, NAM, NMN, cAMP, succinyl-AMP, NADP, GMP, IMP, phosphocholine, *O*-phospho-L-serine, *O*-phospho-L-tyrosine, casein, ATP, GDP and D, L-2-amino-3-phosphonopropionic acid (DL-AP3). Concentration of the substrate used was 5 mM, except for pyridoxal-5′-phosphate, glucose-6-phosphate and pNPP, which were 6 mM, 15 mM and 10 mM respectively. (D) Substrate vs. specific activity plots fit to Michaelis–Menton equation (equation 1) for β-glycerophosphate, α-glycerophosphate and pyridoxal-5′-phosphate (PLP). Plots for XMP and AMP are shown in inset. Activities were measured by estimating the liberated phosphate using Chen's assay (Chen et al., 1956). The plots were generated with GraphPad Prism version 4 (GraphPad software, Inc., San Diego, CA).

gave a K_i value of 0.25 ± 0.02 mM upon fitting the non-linear curves to equation for competitive inhibition (Fig. S2C).

The physiological substrate of PVX_123945, however, remains unknown. It was hypothesized, based on sequence analysis and structure alignment, that PVX_123945 might be a phosphatase specifically hydrolyzing sugar phosphates. Using the prediction, a focused activity screen was devised (Table S1). Thirty-eight substrates were tested to ascertain the substrate specificity profile of the enzyme using a continuous and an end-point assay. Substrates of various sizes and with varying amount of phosphate content were used to understand the broad substrate specificity profile of the enzyme. Intermediate-sized purine and pyrimidine nucleotide monophosphates (their analogs) and phosphorylated sugars, phosphorylated cofactors, phosphorylated metabolites, di-phosphorylated and tri-phosphorylated substrates, small-phosphorylated amino acids and large phosphorylated proteins were tested as a representative set

Table 3
Kinetic constants for putative substrates of PVX_123945.

S.No.	Substrates	K_m (mM)	V_{max} (nmol min^{-1} mg^{-1})	k_{cat} (s^{-1})	k_{cat}/K_m (mM^{-1} s^{-1}) $\times 10^{-3}$
1	β-Glycerophosphate[a]	2.5 ± 0.5	1211 ± 67	0.69	276
2	α-Glycerophosphate[a]	12 ± 3	691 ± 80	0.39	32.8
3	Pyridoxal 5′-phosphate[a]	9 ± 2	1528 ± 140	0.87	96.8
4	Xanthosine 5′-monophosphate[a]	26 ± 2	1331 ± 63	0.76	29.2
5	Adenosine 5′-monophosphate[a]	28 ± 2	913 ± 21	0.52	18.6
6	pNPP[b]	0.6 ± 0.1	3.1 ± 0.1	0.002	3.0

[a] Assay conditions were 50 mM Tris–HCl, pH 7.4, 20 mM $MgCl_2$, and 27 °C. End-point assay was carried out by quenching the reaction at 30 minutes and estimating for liberated phosphate using Chen's method at 820 nm. The concentration of enzyme used was 730 nM.

[b] Assay was carried out by continuously monitoring for pNP formation at 405 nm, at pH 8.0. The concentration of enzyme used was 2.36 μM. The error values indicate standard deviation (S.D.) from triplicate measurements.

(Table S1). It was observed that the enzyme catalyzed the hydrolysis of β-glycerophosphate, α-glycerophosphate, adenosine monophosphate, xanthosine monophosphate, pyridoxal-L phosphate and various sugar phosphates apart from its activity on the artificial substrate p-nitrophenyl phosphate (Fig. 2C). Further, the enzyme showed poor activity on 5′ monophosphorylated nucleotides of guanosine and inosine, 3′ monophosphorylated nucleotide of adenosine, c-AMP, succinyl-AMP, pyrimidine mononucleotides, glucose-1-phosphate, 2,3-bisphosphoglycerate, phosphoenolpyruvate, nucleoside triphosphates, phosphorylated cofactors, nucleoside diphosphates, phosphorylated amino acids and some representative phosphoproteins (Table S1). It was surprising to note that, in spite of the diverse substrate specificity shown by the enzyme, it was capable of discriminating between various substrates as seen in the differential activity toward the various metabolites tested. Further, it should be noted that the enzyme showed highest catalytic efficiency (k_{cat}/K_m) on β-glycerophosphate followed by pyridoxal 5′-phosphate and moderate catalytic efficiency on XMP, AMP and α-glycerophosphate (Fig. 2D and Table 3). However, the significance of activity against these metabolites would necessitate further investigation. It should be noted that β-glycerophosphate has been used as a non-physiological substrate (Olczak et al., 1997; Panara et al., 1994; Penheiter et al., 1997; Torriani, 1960) to test the activity of various phosphatases.

Overall, the results indicate that though the enzyme exhibits phosphatase activity on phosphates of glycerol, pyridoxal and purine nucleotides, the kinetic parameters suggest that the enzyme may indeed differentiate between the metabolite pools presented to it in the cellular milieu.

4. Discussion

Recent observations in the literature suggest that HAD members catalyze various reactions on diverse subset of substrates in spite of having conserved core chemistry (Gohla et al., 2005; Tribble et al., 2006; Guggisberg et al., 2014; Kuznetsova et al., 2006; Srinivasan et al., 2014). PVX_123945 shows conservation of residues with HADs belonging to different subsets. The determinants of substrate specificity in HADs from previous biochemical, structural and bioinformatics studies have not been fully understood. In the light of those observations, it would be interesting to determine the residues that confer the characteristic substrate specificity profile to each member. The experimental results point out that PVX_123945 displays specificity for β-glycerophosphate and pyridoxal 5′-phosphate, with catalytic efficiency for the former being significantly higher. It was indeed intriguing that the enzyme differentiated between α and β-glycerophosphate with 10-fold higher catalytic efficiency for the latter. It should be noted that in most cell types, the physiologically relevant glycerol phosphate is α-glycerophosphate, generated by the action of glycerol kinase on glycerol. To our knowledge, there is no direct metabolic route for the generation of β-glycerophosphate. Examination of the recent literature, however, revealed a study that reported the presence of a phosphotransferase activity on to glycerol associated with a HAD family member (Wang et al., 2010). This protein, referred to as Gtp3, is a small HAD member and is present in the pathway for the biosynthesis of CDP-2 glycerol. The study shows indirect association of a phosphotransferase activity with Gtp3, wherein the γ-phosphate from ATP is transferred to glycerol with the resulting β-glycerophosphate being converted to CDP-2 glycerol by the enzyme Gtp2. The authors also state that the intermediate β-glycerophosphate could not be detected and the formation of the final compound, CDP-2 glycerol from glycerol, ATP and CTP suggests a phosphotransferase activity for the HAD enzyme Gtp3. As PVX_123945 exhibits phosphatase activity on β-glycerophosphate, we attempted to examine the ATP hydrolyzing activity in the presence of glycerol by this enzyme. We used a coupled enzyme assay involving pyruvate kinase and lactate dehydrogenase but failed to detect significant ATP hydrolyzing activity, both in the presence and absence of glycerol (data not shown). Therefore, the high catalytic efficiency of PVX-123945 on β-glycerophosphate cannot, at present, be assigned a physiological role.

In a recent publication it has been demonstrated that PfHAD1, the *P. falciparum* homolog of PVX_111055, is a sugar phosphate phosphatase regulating the methylerythritol phosphate pathway in the malaria parasite (Guggisberg et al., 2014). Recombinant PfHAD1 was assayed with 25 different sugar phosphates with the maximum activity shown for fructose-1-phosphate. When the structures of PVX_123945 (PDB ID: 2B30) and PfHAD1 (PDB ID: 4QJB) were compared, they showed good structural superposition with a root-mean square deviation of 1.37 Å in spite of low sequence identity (29%) between the two proteins. However, as has been depicted in Fig. 1A, the overall fold conservation across various HAD superfamily sugar hydrolases is quite high in spite of low sequence similarity. It should be noted that PfHAD1 exhibited catalytic efficiency on β-glycerophosphate that was comparable with fructose-1-phosphate, mannose-6-phosphate and glyceraldehyde-3-phosphate. The PVX_123945 enzyme however, shows significantly higher catalytic efficiency for β-glycerophosphate as compared to the other three substrates.

It has been amply demonstrated in literature that enzymes displaying broad substrate specificity are reservoirs for enzyme evolution. Initial hypothesis by Jensen (1976) and O'Brien and Herschlag (1999) and subsequent demonstration by Babbitt and Gerlt (for enolase superfamily) (Babbitt and Gerlt, 1997; Gerlt and Babbitt, 2001; Gerlt et al., 2005; Schmidt et al., 2003) and by Schofield (for crotonase superfamily) (Hamed et al., 2008) has shown that enzymes displaying broad substrate specificity are reservoirs for evolution of new and specific function. Catalytic evolution and functional diversification in the mechanistically diverse HAD superfamily have also been extensively discussed in literature (Burroughs et al., 2006; Glasner et al., 2006). A recent review elaborates on enzyme promiscuity as an engine of evolutionary innovation in HAD superfamily phosphatases (Pandya et al., 2014). Further, in vitro evolution studies on enzymes displaying promiscuous activity by Tawfik's group (Aharoni et al., 2005; Gupta and Tawfik, 2008; Khersonsky et al., 2006; Peisajovich and Tawfik, 2007) and Arnold's group (Bloom et al., 2007) has amply demonstrated that substrate promiscuity is an essential requirement for enzyme evolution. It has been shown that the plasticity of enzyme active site designed for acting on multiple substrates with average/poor catalytic efficiency renders it easy for enzymes to acquire a novel function with a few amino acid changes without compromising the original function for which it had evolved over millions of years (called neutral drift) (Khersonsky et al., 2006; Yoshikuni et al., 2006).

This leads us to speculate that the enzyme PVX123945 might be a reservoir for evolution of novel functional variants by gene duplication events (Aharoni et al., 2005; O'Brien and Herschlag, 1999). This promiscuous form of the enzyme might be a progenitor or evolutionary node/ node-intermediate in the evolution and fine-tuning of specific activities. These reservoirs may be particularly relevant to a pathogen that has to devise novel strategies to evade the host immune response and be successful as an effective pathogen.

5. Conclusions

The study is the first attempt at annotating the function of a hypothetical protein belonging to HAD superfamily of hydrolases in *P. vivax*. Using distant homology sequence searches and structure comparison, the study predicts the protein PVX_123945 to be a phosphatase. Using biochemical and kinetic studies, the in silico predictions are validated and it is demonstrated that the protein is a broad specificity phosphatase catalyzing the hydrolysis of

β-glycerophsphate, pyridoxal-L-phosphate, xanthosine monophosphate, adenosine monophosphate and α-glycerophosphate with Mg^{2+} as the most preferred divalent cation.

Acknowledgments

Financial support for this research came from Department of Science and Technology and Department of Biotechnology, India. BS was a recipient of senior research fellowship from the Council of Scientific and Industrial Research (CSIR). LKN and AS are recipients of Junior and Senior Research Fellowships from CSIR. The expression clone was a kind gift from the Structural Genomics Consortium for Pathogenic Protozoan (SGPP).

Appendix: Supplementary material

Supplementary data to this article can be found online at doi:10.1016/j.endend.2013.05.004.

References

Acharya, P., Pallavi, R., Chandran, S., Dandavate, V., Sayeed, S.K., Rochani, A., et al., 2011. Clinical proteomics of the neglected human malarial parasite Plasmodium vivax. PLoS ONE 6, e26623.
Aharoni, A., Gaidukov, L., Khersonsky, O., McQ Gould, S., Roodveldt, C., Tawfik, D.S., 2005. The 'evolvability' of promiscuous protein functions. Nat. Genet. 37, 73–76.
Allen, K.N., Dunaway-Mariano, D., 2004. Phosphoryl group transfer: evolution of a catalytic scaffold. Trends Biochem. Sci. 29, 495–503.
Altschul, S.F., Madden, T.L., Schaffer, A.A., Zhang, J., Zhang, Z., Miller, W., et al., 1997. Gapped BLAST and PSI-BLAST: a new generation of protein database search programs. Nucleic Acids Res. 25, 3389–3402.
Babbitt, P.C., Gerlt, J.A., 1997. Understanding enzyme superfamilies. Chemistry As the fundamental determinant in the evolution of new catalytic activities. J. Biol. Chem. 272, 30591–30594.
Bernstein, F.C., Koetzle, T.F., Williams, G.J., Meyer, E.F., Jr., Brice, M.D., Rodgers, J.R., et al., 1977. The Protein Data Bank: a computer-based archival file for macromolecular structures. J. Mol. Biol. 112, 535–542.
Bloom, J.D., Romero, P.A., Lu, Z., Arnold, F.H., 2007. Neutral genetic drift can alter promiscuous protein functions, potentially aiding functional evolution. Biol. Direct. 2, 17.
Bradford, M.M., 1976. A rapid and sensitive method for the quantitation of microgram quantities of protein utilizing the principle of protein-dye binding. Anal. Biochem. 72, 248–254.
Burroughs, A.M., Allen, K.N., Dunaway-Mariano, D., Aravind, L., 2006. Evolutionary genomics of the HAD superfamily: understanding the structural adaptations and catalytic diversity in a superfamily of phosphoesterases and allied enzymes. J. Mol. Biol. 361, 1003–1034.
Carlton, J.M., Adams, J.H., Silva, J.C., Bidwell, S.L., Lorenzi, H., Caler, E., et al., 2008. Comparative genomics of the neglected human malaria parasite Plasmodium vivax. Nature 455, 757–763.
Chen, P.S., Toribara, T.Y., Warner, H., 1956. Microdetermination of phosphorus. Anal. Chem. 28, 1756–1758.
Eisenstein, E., Gilliland, G.L., Herzberg, O., Moult, J., Orban, J., Poljak, R.J., et al., 2000. Biological function made crystal clear – annotation of hypothetical proteins via structural genomics. Curr. Opin. Biotechnol. 11, 25–30.
Frech, C., Chen, N., 2011. Genome comparison of human and non-human malaria parasites reveals species subset-specific genes potentially linked to human disease. PLoS Comput. Biol. 7, e1002320.
Galperin, M.Y., 2001. Conserved 'hypothetical' proteins: new hints and new puzzles. Comp. Funct. Genomics 2, 14–18.
Gardner, M.J., Hall, N., Fung, E., White, O., Berriman, M., Hyman, R.W., et al., 2002. Genome sequence of the human malaria parasite Plasmodium falciparum. Nature 419, 498–511.
Gerlt, J.A., Babbitt, P.C., 2001. Divergent evolution of enzymatic function: mechanistically diverse superfamilies and functionally distinct suprafamilies. Annu. Rev. Biochem. 70, 209–246.
Gerlt, J.A., Babbitt, P.C., Rayment, I., 2005. Divergent evolution in the enolase superfamily: the interplay of mechanism and specificity. Arch. Biochem. Biophys. 433, 59–70.
Glasner, M.E., Gerlt, J.A., Babbitt, P.C., 2006. Evolution of enzyme superfamilies. Curr. Opin. Chem. Biol. 10, 492–497.
Gohla, A., Birkenfeld, J., Bokoch, G.M., 2005. Chronophin, a novel HAD-type serine protein phosphatase, regulates cofilin-dependent actin dynamics. Nat. Cell Biol. 7, 21–29.
Guex, N., Peitsch, M.C., 1997. SWISS-MODEL and the Swiss-PdbViewer: an environment for comparative protein modeling. Electrophoresis 18, 2714–2723.
Guggisberg, A.M., Park, J., Edwards, R.L., Kelly, M.L., Hodge, D.M., Tolia, N.H., et al., 2014. A sugar phosphatase regulates the methylerythritol phosphate (MEP) pathway in malaria parasites. Nat. Comm. 5, 4467.
Gupta, R.D., Tawfik, D.S., 2008. Directed enzyme evolution via small and effective neutral drift libraries. Nat. Methods 5, 939–942.
Hamed, R.B., Batchelar, E.T., Clifton, I.J., Schofield, C.J., 2008. Mechanisms and structures of crotonase superfamily enzymes–how nature controls enolate and oxyanion reactivity. Cell. Mol. Life Sci. CMLS 65, 2507–2527.
Holm, L., Park, J., 2000. DaliLite workbench for protein structure comparison. Bioinformatics 16, 566–567.
Huang, H., Patskovsky, Y., Toro, R., Farelli, J.D., Pandya, C., Almo, S.C., et al., 2011. Divergence of structure and function in the haloacid dehalogenase enzyme superfamily: bacteroides thetaiotaomicron BT2127 is an inorganic pyrophosphatase. Biochemistry 50, 8937–8949.
Jensen, R.A., 1976. Enzyme recruitment in evolution of new function. Annu. Rev. Microbiol. 30, 409–425.
Jones, D.T., 1999. GenTHREADER: an efficient and reliable protein fold recognition method for genomic sequences. J. Mol. Biol. 287, 797–815.
Khersonsky, O., Roodveldt, C., Tawfik, D.S., 2006. Enzyme promiscuity: evolutionary and mechanistic aspects. Curr. Opin. Chem. Biol. 10, 498–508.
Kumar, S., Tamura, K., Nei, M., 1994. MEGA: molecular evolutionary genetics analysis software for microcomputers. Computer applications in the biosciences. CABIOS 10, 189–191.
Kuznetsova, E., Proudfoot, M., Gonzalez, C.F., Brown, G., Omelchenko, M.V., Borozan, I., et al., 2006. Genome-wide analysis of substrate specificities of the Escherichia coli haloacid dehalogenase-like phosphatase family. J. Biol. Chem. 281, 36149–36161.
Laemmli, U.K., 1970. Cleavage of structural proteins during the assembly of the head of bacteriophage T4. Nature 227, 680–685.
Lu, Z., Dunaway-Mariano, D., Allen, K.N., 2005. HAD superfamily phosphotransferase substrate diversification: structure and function analysis of HAD subclass IIB sugar phosphatase BT4131. Biochemistry 44, 8684–8696.
Lu, Z., Dunaway-Mariano, D., Allen, K.N., 2011. The X-ray crystallographic structure and specificity profile of HAD superfamily phosphohydrolase BT1666: comparison of paralogous functions in B. thetaiotaomicron. Proteins 79, 3099–3107.
Mendis, K., Sina, B.J., Marchesini, P., Carter, R., 2001. The neglected burden of Plasmodium vivax malaria. Am. J. Trop. Med. Hyg. 64, 97–106.
Morris, G.M., Huey, R., Olson, A.J., 2008. Using AutoDock for ligand-receptor docking, Current protocols in bioinformatics/editorial board, Andreas D Baxevanis [et al], Chapter 8, Unit 8.14.
Nguyen, C.M., Lee, H.S., Cho, Y., Lee, J.H., Ha, S.C., Hwang, H.Y., et al., 2008. Crystallization and preliminary X-ray studies of TON_0559, a putative member of the haloacid dehalogenase (HAD) superfamily from Thermococcus onnurineus NA1. Protein Pept. Lett. 15, 235–237.
Notredame, C., Higgins, D.G., Heringa, J., 2000. T-Coffee: a novel method for fast and accurate multiple sequence alignment. J. Mol. Biol. 302, 205–217.
O'Brien, P.J., Herschlag, D., 1999. Catalytic promiscuity and the evolution of new enzymatic activities. Chem. Biol. 6, R91–R105.
Olczak, M., Watorek, W., Morawiecka, B., 1997. Purification and characterization of acid phosphatase from yellow lupin (Lupinus luteus) seeds. Biochim. Biophys. Acta 1341, 14–25.
Panara, F., Angiolillo, A., Di Rosa, I., Fagotti, A., Contenti, S., Simoncelli, F., et al., 1994. Purification and some properties of a Mg(2+)-activated acid phosphatase from rat testis. Int. J. Biochem. 26, 885–890.
Pandya, C., Farelli, J.D., Dunaway-Mariano, D., Allen, K.N., 2014. Enzyme promiscuity: engine of evolutionary innovation. J. Biol. Chem. 289, 30229–30236.
Peisajovich, S.G., Tawfik, D.S., 2007. Protein engineers turned evolutionists. Nat. Methods 4, 991–994.
Penheiter, A.R., Duff, S.M., Sarath, G., 1997. Soybean root nodule acid phosphatase. Plant Physiol. 114, 597–604.
Schmidt, D.M., Mundorff, E.C., Dojka, M., Bermudez, E., Ness, J.E., Govindarajan, S., et al., 2003. Evolutionary potential of (beta/alpha)8-barrels: functional promiscuity produced by single substitutions in the enolase superfamily. Biochemistry 42, 8387–8393.
Srinivasan, B., Balaram, H., 2007. ISN1 nucleotidases and HAD superfamily protein fold: in silico sequence and structure analysis. In Silico Biol. 7, 187–193.
Srinivasan, B., Forouhar, F., Shukla, A., Sampangi, C., Kulkarni, S., Abashidze, M., et al., 2014. Allosteric regulation and substrate activation in cytosolic nucleotidase II from Legionella pneumophila. FEBS J. 281, 1613–1628.
Torriani, A., 1960. Influence of inorganic phosphate in the formation of phosphatases by Escherichia coli. Biochim. Biophys. Acta 38, 460–469.
Tribble, G.D., Mao, S., James, C.E., Lamont, R.J., 2006. A Porphyromonas gingivalis haloacid dehalogenase family phosphatase interacts with human phosphoproteins and is important for invasion. Proc. Natl. Acad. Sci. U.S.A. 103, 11027–11032.
Wang, Q., Xu, Y., Perepelov, A.V., Xiong, W., Wei, D., Shashkov, A.S., et al., 2010. Characterization of the CDP-2-glycerol biosynthetic pathway in Streptococcus pneumoniae. J. Bacteriol. 192, 5506–5514.
Yoshikuni, Y., Ferrin, T.E., Keasling, J.D., 2006. Designed divergent evolution of enzyme function. Nature 440, 1078–1082.